

Consistency-based Abductive Reasoning over Perceptual Errors of Multiple Pre-trained Models in Novel Environments

Mario Leiva¹, Noel Ngu², Joshua Shay Kricheli^{2,3}, Aditya Taparia², Ransalu Senanayake², Paulo Shakarian³, Nathaniel Bastian⁴, John Corcoran⁵ and Gerardo Simari¹

¹Department of Computer Science and Engineering, Universidad Nacional del Sur and Institute for Computer Science and Engineering, Bahía Blanca, Argentina

²Arizona State University, Tempe, AZ USA

³Syracuse University, Syracuse, NY USA

⁴United States Military Academy, West Point, NY USA

⁵U.S. Department of Defense, Arlington, VA USA

mario.leiva@cs.uns.edu.ar, {nngu2, jkrichel, ataparia, ransalu}@asu.edu, pashakar@syr.edu, nathaniel.bastian@westpoint.edu, john.corcoran.ctr@darpa.mil and gis@cs.uns.edu.ar

Abstract

The deployment of pre-trained perception models in novel environments often leads to performance degradation due to distributional shifts. Although recent artificial intelligence approaches for metacognition use logical rules to characterize and filter model errors, improving precision often comes at the cost of reduced recall. This paper addresses the hypothesis that leveraging multiple pre-trained models can mitigate this recall reduction. We formulate the challenge of identifying and managing conflicting predictions from various models as a consistency-based abduction problem. The input predictions and the learned error detection rules derived from each model are encoded in a logic program. We then seek an abductive explanation—a subset of model predictions—that maximizes prediction coverage while ensuring the rate of logical inconsistencies (derived from domain constraints) remains below a specified threshold. We propose two algorithms for this knowledge representation task: an exact method based on Integer Programming (IP) and an efficient Heuristic Search (HS). Through extensive experiments on a simulated aerial imagery dataset featuring controlled, complex distributional shifts, we demonstrate that our abduction-based framework outperforms individual models and standard ensemble baselines, achieving, for instance, average relative improvements of approximately 13.6% in F1-score and 16.6% in accuracy across 15 diverse test datasets when compared to the best individual model. Our results validate the use of consistency-based abduction as an effective mechanism to robustly integrate knowledge from multiple imperfect reasoners in challenging, novel scenarios.

1 Introduction

The use of pre-trained models is very common in tasks that require perception data, such as classification and object detection in images and video (Han et al. 2021; Parisi et al. 2022). Another scenario in which differences arise is when we know we will be deploying in different environments because we are using the models that we have available—we refer to these issues as *deployment in novel environments*. As a specific example, consider emergency response,

where perception models examining a disaster must contend with unforeseen environmental changes even when trained on data for a similar region. Another example is an NGO providing aid to a remote location where training data was unavailable. In both cases, we can be assured that the environment in which the perception models operate is *novel* with respect to what they are trained on.

Following the renewed interest in metacognitive artificial intelligence (AI) (Wei et al. 2024; Johnson et al. 2024), recent work (Xi et al. 2024; Kricheli et al. 2024; Lee et al. 2024; Shakarian, Simari, and Bastian 2025) addresses the problem of deploying a single pre-trained model in novel environments via so-called *error detection and correction rules* (EDCR) that allow to characterize the errors made by a model in the form of logical rules. The authors show that such rules can be learned from data, and experiments in a geospatial domain show that applying them has the effect of increasing performance in terms of precision at the cost of a reduction in recall. We note that this result is obtained despite both the model and rules being learned on data that differs from the distribution at test time.

In this work, our working hypothesis is that by deploying more than one model we are able to at least partially address this drawback; this is the same idea behind standard approaches in machine learning for developing ensembles of models, but our approach goes beyond such standard practices since we apply novel metacognitive AI techniques. In particular, as shown in Figure 1, we leverage existing rule learning techniques to derive a logic program consisting of metacognitive rules across a set of perception models, and frame the task of identifying errors across all models as a *consistency-based abduction problem*. We then show that such error identification problems can be posed as integer programs, and provide a scalable heuristic algorithm to solve the abductive reasoning task. Noteworthy in our approach is that the logic program is created by EDCR rules learned for each perceptual model based on their training data—so there is no a-priori knowledge of test data (i.e., no leakage). Further, the rules for the individual models are learned inde-

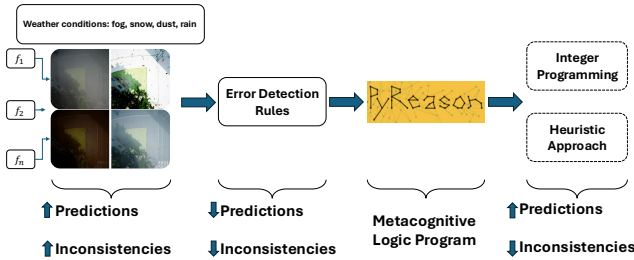


Figure 1: Overview of our Consistency-based Abductive Reasoning Approach. Potentially noisy and conflicting predictions from multiple pre-trained models (f_1, f_2, \dots, f_n) operating in novel environments are processed through a Metacognition Logic Program (incorporating learned error characteristics and executed via PyReason) to identify plausible assertions. Then, one of two proposed abductive methods—exact Integer Programming approach or a scalable Heuristic Search algorithm—is employed. Both aim to maximize the set of accepted valid predictions while ensuring overall inconsistency remains below a predefined threshold δ .

pendently for each other—so we assume there is no existing knowledge of how the models perform together.

Finally, we present a thorough experimental evaluation using an extended, highly-controlled aerial imagery dataset with diverse distributions (Ngu et al. 2025). Our results demonstrate that our abductive-based reasoning approach—by effectively managing inconsistencies while maximizing predictions—achieves superior performance compared to individual models across numerous test datasets.

2 Related Work

This work is closely related to (Xi et al. 2024), where Error Detection and Correction rules are introduced. The main difference with our approach is that they only consider a single model. As we discuss below, here we only leverage error detection rules, though the approach can easily accommodate the use of correction rules as well.

Abductive learning (ABL) (Dai et al. 2019) also leverages abduction to reduce perception errors and, like our approach, relies on some domain knowledge (for instance, we require knowledge about consistent predictions). However, ABL uses this to improve performance based on model training and assumes that the test environment is not entirely novel. In this work, we relax both assumptions and use abduction only at test time. We note that a follow-on study, called “ABL with new concepts” (ABL_{nc}) (Huang et al. 2023) extends ABL—in a manner similar to EDCR—with the ability to identify previously “unknown” concepts, which EDCR (Xi et al. 2024) was also shown to have. Like ABL, this approach is also focused on using abduction at model training and not inference. In this work, we do not extend the concept scheme (though approaches like ABL/ ABL_{nc} , EDCR, and HDC could all potentially be helpful) but rather change the distribution of perceptual data by which such concepts are extracted. We note that early work on abduction often focused on the diagnosis of errors and faults (Poole 1989); however, to our knowledge this has not been applied to perception tasks at test time. This early work

inspired our use of abduction to identify perception errors.

Recently, a concept known as “test-time training” (TTT) (Sun et al. 2020) has gained traction in the machine learning literature and has shown importance in reasoning tasks as well (Akyürek et al. 2024). In this approach, the neural model is trained in a manner such that it performs self-supervised training during test time to improve inference. While this shows ability to improve out-of-distribution results, it is also a method designed to improve model training, and was noted to have limitations based on the classes used in the self-supervised training. We note that such a TTT model could be treated as any other pre-trained model in our framework, and we can even envision different variants of TTT (e.g., with different strategies for the self-supervised portion) better working together by leveraging our results.

Finally, in (Sutor et al. 2022), the authors also explore combining a set of pre-trained models using hyperdimensional computing (HDC). However, their method relies on having a set of training samples from the same target distribution as the test set, enabling the joint training of an HDC “gluing” module. In contrast, here we assume that data from the same distribution as the test set is unavailable and that the models are trained independently. Furthermore, their method depends on the output layers of the neural networks and lacks explainability, unlike our rule-based approach.

3 Consistency-based Abduction

We consider the problem of object identification for a given set of perception data Ω (Cheng and Han 2016) and assume the availability of a set η of perception models $\mathcal{F} = \{f_1, f_2, \dots, f_\eta\}$, where each model generates a set of predictions over a shared set of m object classes $\mathcal{C} = \{c_1, \dots, c_m\}$. Since multiple models may generate predictions for the same object, inconsistencies between predictions naturally arise when there is disagreement. To address the challenge of managing predictions from multiple perception models, the EDCR framework (Xi et al. 2024) provides a principled approach to learning error detection rules that can improve the reliability of a model’s predictions for a particular class, establishing a precision-recall trade-off. A key aspect of this process is the parameter $\epsilon \in [0, 1]$, which defines the maximum allowable reduction in recall (based on training data) when constructing these rules for specific model-class pairs $(f, c) \in \mathcal{F} \times \mathcal{C}$. By introducing ϵ , EDCR ensures that rule selection is guided by a balance between the two performance metrics for a particular model and class. By tuning ϵ , it is possible to filter out predictions from a model for a class, which reduces inconsistencies between all predictions from all models. However, this may also result in a reduction in the total number of valid predictions (i.e., lower precision).

3.1 Problem Definition

Our objective can thus be framed as the maximization of the total number of predictions across all models, subject to the constraint that the inconsistencies remain below a threshold, which we call $\delta \in [0, 1]$. Additionally, the solution requires selecting an optimal value for the ϵ parameter, as well as a

subset of model-class pairs (f, c) to include in the evaluation. We now present the general formal problem.

Optimization Problem. Given the following:

- $\mathcal{P} = \mathcal{F} \times \mathcal{C}$: The set of all model-class pairs;
- $\epsilon \in [0, 1]$: Recall reduction threshold;
- $\text{Pred}(\epsilon, \mathcal{P}')$: The number of predictions for a subset of pairs $\mathcal{P}' \subseteq \mathcal{P}$ given threshold ϵ ;
- $\text{Inc}(\mathcal{P}')$: The percentage of inconsistencies among the predictions for pairs in \mathcal{P}' ;

The optimization problem can be expressed as:

$$\max_{\epsilon, \mathcal{P}'} \text{Pred}(\epsilon, \mathcal{P}'),$$

subject to:

$$\text{Inc}(\mathcal{P}') \leq \delta, \quad \epsilon \in [0, 1], \quad \delta \in [0, 1], \quad \mathcal{P}' \subseteq \mathcal{P},$$

where:

$$\begin{aligned} \text{Pred}(\epsilon, \mathcal{P}') &= \sum_{(f, c) \in \mathcal{P}'} |\{\omega \in \Omega \mid f(\omega) = c \text{ given } \epsilon\}|; \\ \text{Inc}(\mathcal{P}') &= \frac{|\{\omega \in \Omega \mid \exists (f_i, c_i), (f_j, c_j) \in \mathcal{P}' : f_i(\omega) \neq f_j(\omega)\}|}{|\Omega|}. \end{aligned}$$

The constraints above respectively ensure that inconsistencies remain within the acceptable threshold, valid values for the recall reduction threshold and percentage of inconsistencies parameters are used, and a subset of model-class pairs is selected. This can thus be viewed as an abductive reasoning problem (Gabbay and Smets 2013) in which the space of hypotheses is the set of all possible model-class pairs. Next, we show how this problem can be tackled by leveraging error detection rules encoded in logic programs.

3.2 Error Detection Rule Learning and Logical Inferences

In order to address model inaccuracies in object detection, we use the set of rule-based mechanisms for detecting errors, called *Error Detection and Correction Rules* (EDCR) presented in (Xi et al. 2024). Such rules leverage conditions learned from training sets to characterize model errors. Each class $c \in \mathcal{C}$ is assigned a detection rule that determines if the predicted class for a sample sequence ω is likely erroneous. Let the predicted class be represented by $\text{pred}_c(\omega)$, which is true if the model predicts class c for ω . For a given class c , detection rules use a set of conditions DC_c , defined over input characteristics, to determine if a sample is likely misclassified. The detection rule for a class c is defined as:

$$\text{error}_c(\omega) \leftarrow \text{pred}_c(\omega) \wedge \bigvee_{\text{cond} \in DC_c} \text{cond}(\omega), \quad (1)$$

where $\text{cond} \in DC_c$ denotes specific conditions that, when satisfied, indicate that the model’s prediction may be incorrect. For detection, we aim to select DC_c from a predefined set of conditions so as to maximize detection precision with minimal reduction in recall, denoted by the value of the ϵ

parameter. Before recalling the detection rule-learning algorithm, we introduce the essential elements used in rule construction: POS and NEG. Each of these elements quantifies specific conditions across the samples: POS represents the count of samples for which both the rule’s body and head are satisfied, indicating correct classifications under the current conditions, while NEG, in contrast, is the number of samples satisfying the rule’s body but not the head, signaling cases where conditions lead to misclassifications. Together, these elements enable the computation of key metrics—such as support and confidence—that inform the rule-learning process, ensuring that only conditions contributing to accurate classification are retained.

The *DetRuleLearn* algorithm in (Xi et al. 2024) builds on these foundations to iteratively learn error detection rules for a specific class. It aims to identify a subset of conditions (DC_c) that maximize precision while ensuring that the recall reduction does not exceed the threshold ϵ . Starting with an empty rule set, the algorithm iteratively selects the condition that provides the greatest improvement in error detection (maximizing POS) without violating the recall constraint. The process continues until no valid conditions remain. Leveraging submodular optimization, the algorithm achieves an efficient approximation of the optimal solution, balancing error detection precision and recall preservation. For the full details of the algorithm, we refer the reader to (Xi et al. 2024). We note that we apply *DetRuleLearn* to each model independently on its own training data to avoid the assumption of prior knowledge of model ensemble performance. We can think of the rules learned for a specific model as a formal representation of its performance characteristics on that dataset—akin to a model card represented as a logic program (i.e. a “smart model card”).

3.3 Logical Inferences and Outcomes of the Deduction Process

We now provide the building blocks needed to formulate our consistency-based abduction inference approach.

Language. We use a simple first-order language as per (Xi et al. 2024) and later extended in (Kricheli et al. 2024). However, we will add a superscript j to the predicates denoting the model making the prediction (as we use multiple models in this case). Further, we shall use constants that represent objects, as opposed to samples; so, we can think of a given reasoning process occurring for a single sample that has multiple objects perceived by the perception models. As mentioned above, we assume a collection \mathcal{F} of η perception models; though we assume each of these models is parameterized (e.g., model f_j is associated with parameters θ_j), we omit the parameter notation for clarity. In this language, objects are represented by constant symbols (ω). We also define a collection of $|\mathcal{C}| \cdot |\mathcal{F}| = m\eta$ “condition” unary predicates $\text{cond}_1^1, \dots, \text{cond}_m^1$ (i.e., cond_i^j can be thought of as the version of condition i associated with model j). Such predicates can be thought of as associated with each object, and can be either true or false—these conditions can potentially lead to failure, and learning algorithms can identify

which ones lead to failure for a given prediction. We also define unary predicates for each class c and model f : pred_c^f and error_c^f as follows:

- $\text{pred}_c^f(\omega)$: True iff model f predicts class c for object ω , i.e., $\text{pred}_c^f(\omega) \iff f(\omega) = c$.
- $\text{error}_c^f(\omega)$: True iff an EDCR rule concludes that model f_j erroneously predicted class c for object ω , i.e., $\text{error}_c^f(\omega) \iff f(\omega) = c$ and $gt(\omega) \neq c$, where gt is the ground truth oracle function.

Rules. We use Π to denote the set of rules for each model-class pair, seeking to detect if a prediction by the corresponding model is not valid for the corresponding class. Thus, for each model-class pair (f, c) , we have a rule:

$$\text{error}_c^f(\omega) \leftarrow \text{pred}_c^f(\omega) \wedge \left(\bigvee_{\text{cond} \in DC_c^f} \text{cond}(\omega) \right). \quad (2)$$

Logic Programs. For the deductive process, we leverage the semantics of annotated logic (Kifer and Subrahmanian 1992) as implemented by PyReason (Aditya et al. 2023). In this work, we simplify the representation by omitting annotations, treating atoms as either true (equivalent to an annotation of $[1, 1]$) or false (using strong negation “ \neg ”, equivalent to an annotation of $[0, 0]$). The open-world paradigm is represented by the annotation $[0, 1]$, indicating complete uncertainty. The logic program Π includes facts derived from each perception model, enabling the deduction of object-class assignments. We use $\Gamma^*(\Pi)$, slightly adapted from (Kifer and Subrahmanian 1992), to refer to the set of all literals concluded by Π in its minimal model, which includes all atoms determined to be either true or false. PyReason serves as the platform for executing the logic program, allowing for efficient reasoning over rules.

Unique Name Assumption. We assume that all constants have a unique name—for example, if an object is assigned the name ω_5 , then it will receive the same name by all models. Using our notation, if Π contains facts $\text{pred}_{c_3}^{f_2}(\omega_5)$ and $\text{pred}_{c_6}^{f_7}(\omega_5)$, then some object ω_5 was perceived by both models f_2 and f_7 and assigned class c_3 by f_2 and class c_6 by f_7 (i.e., $f_2(\omega_5) = c_3$ and $f_7(\omega_5) = c_6$).

Integrity Constraints. We assume the availability of domain knowledge indicating that objects cannot belong to certain pairs of classes at once. We denote such incompatible classes with pairs (c, c') , where $c, c' \in \mathcal{C}$, and the set of such integrity constraints with IC .

Prima Facie Class Assignment We now formally define the outcome of the deduction process that we leverage.

Definition 3.1. *Prima Facie Class Assignment (PFCA) of class c . Let Π be a logic program with rules over models \mathcal{F} and classes \mathcal{C} . Object ω is assigned to class $c \in \mathcal{C}$ in a prima*

facie class assignment (PFCA) by program Π if and only if there exists model $f_i \in \mathcal{F}$ such that:

$$\text{pred}_c^{f_i}(\omega) \in \Gamma^*(\Pi) \wedge \text{error}_c^{f_i}(\omega) \notin \Gamma^*(\Pi).$$

We can use the results of the deductive process to determine the results associated with a classification task. Given a sample, let us assume that $\Omega = \{\omega_1, \dots, \omega_N\}$ represents the union of all objects returned by any of f_1, \dots, f_n . Under prima facie class assignment, we can build the following set of object-class pairs:

$$\{(\omega, c) \mid \omega \in \Omega \wedge \text{pfca}_c(\omega) \in \Gamma^*(\Pi)\}.$$

This constitutes a set of objects assigned to various classes. The concept of Prima Facie Class Assignment (PFCA) represents a foundational step in the deductive classification process. It assigns an object ω to a class c if at least one model f_i predicts c for ω without marking it as erroneous. For example, consider a scenario where object ω_1 is evaluated by three models f_1, f_2, f_3 . Model f_1 predicts class “vehicle” ($\text{pred}_{\text{vehicle}}^{f_1}(\omega_1)$) with no error flagged ($\text{error}_{\text{vehicle}}^{f_1}(\omega_1) \notin \Gamma^*(\Pi)$), while f_2 and f_3 do not predict “vehicle” or flag any errors. In this case, ω_1 is assigned to class “vehicle” under PFCA. The PFCA set is particularly important because it captures the most general set of object-class pairs, allowing for a high degree of flexibility in evaluations. However, due to its generality, it inherently includes inconsistencies, making it the baseline for constructing more refined sets with stricter consistency rules.

4 Solution Approaches

To address the optimization problem of maximizing assignments while minimizing conflicts under a given inconsistency threshold, we propose two complementary approaches: an *integer programming-based method* and a *heuristic algorithm*. The former is a formulation based on a mathematical optimization model, guaranteeing globally optimal solutions by leveraging exact solvers. However, this method can be computationally expensive for large instances. In contrast, the heuristic approach employs an iterative, approximate strategy to efficiently explore the solution space, providing scalable performance.

4.1 Integer Program (IP) Formulation

Intuitively, given a set $assigns$ of objects assigned to various classes, a set of inconsistencies IC , the union of all objects returned by any model $\Omega = \{\omega_1, \dots, \omega_N\}$, and a threshold $\delta \in [0, 1]$ for the maximum allowed conflicts, we want to find a set $assigns_{opt} \subseteq assigns$ that maximizes the total number of assignments while minimizing conflicts. Formally, this can be expressed as

$$\max \sum_{\omega \in \Omega} \sum_{c \in \mathcal{C}} A_{c, \omega},$$

subject to:

$$\sum_{\omega \in \Omega} \sum_{(c, c') \in IC} Con_{\omega, (c, c')} \leq \delta,$$

where $A_{c,\omega}$ is a binary variable indicating whether object ω is assigned to class c , $Con_{\omega,(c,c')}$ is a binary variable indicating a conflict between assignments c and c' for object ω .

We further define the following constants and variables: $pred_{f,c,\omega}$ is a constant set to 1 if $(\omega, c) \in assigns$ and $pred_c^f(\omega) \in \Gamma^*(\Pi)$, 0 otherwise; variable $Elim_{f,c} \in \{0, 1\}$ indicates whether predictions from model f for class c are excluded; and $X_{\omega,f,c} \in \{0, 1\}$ is a variable that indicates whether object ω is considered for model f and class c .

We can now present the set of constraints. First, for each f, c, ω we have constraints of the form:

$$X_{\omega,f,c} \leq 1 - Elim_{f,c} \quad (3)$$

$$X_{\omega,f,c} \cdot pred_{f,c,\omega} \leq A_{c,\omega} \quad (4)$$

Next, for each c, ω we have:

$$A_{c,\omega} \leq \sum_f X_{\omega,f,c} \cdot pred_{f,c,\omega} \quad (5)$$

For each $\omega \in \Omega, (c, c') \in IC$:

$$A_{c,\omega} + A_{c',\omega} - 1 \leq Con_{\omega,(c,c')} \quad (6)$$

for each ω , we have:

$$\sum_{c \in \mathcal{C}} A_{c,\omega} \geq 1 \quad (7)$$

Finally:

$$\sum_{\omega \in \Omega} \sum_{(c,c') \in IC} Con_{\omega,(c,c')} \leq \delta \quad (8)$$

They respectively ensure the elimination of invalid predictions, consistency between predictions and assignments, upper bounds on assignments per object, that conflicts are adequately managed, that each object is assigned at least one class, and that the global conflict threshold holds.

The IP formulation described by Equations (3)–(8) translates into a model with a number of variables and constraints dependent on the number of unique objects (N), models ($|\mathcal{F}|$), classes ($|\mathcal{C}|$), and integrity constraints ($|IC|$). Specifically, the IP model involves decision variables for assignments ($A_{c,\omega}$), conflict indicators ($Con_{\omega,(c,c')}$), model-class eliminations ($Elim_{f,c}$), and object consideration ($X_{\omega,f,c}$). The total number of variables is primarily driven by the $N \times \mathcal{F} \times \mathcal{C}$ term (associated with $X_{\omega,f,c}$), resulting in an overall count in the order of $O(N|\mathcal{F}||\mathcal{C}|)$. Similarly, the number of constraints also scales in the order of $O(N|\mathcal{F}||IC|)$.

From a knowledge representation and reasoning perspective, while solving such IP instances is NP-hard in the worst case, the specific structure of our consistency-based abduction problem often lends itself to relatively efficient resolution in practice. Our IP formulation is characterized by *binary decision variables*, a *linear objective function* (maximizing valid assignments), and a set of *linear constraints*. Many of these constraints exhibit a degree of *locality* (e.g., defining conflicts $Con_{\omega,(c,c')}$ based on assignments $A_{c,\omega}$ for the same object ω , or linking model-class considerations $X_{\omega,f,c}$ to overall assignments). This structured nature, which demonstrated efficient performance within our specific experimental configuration, often allows for practical solutions to be found within reasonable timeframes for problems of the scale explored in our experiments.

Algorithm 1 Heuristic Search (HS) for Prediction Optimization

```

1: Input:
2:    $P_{raw}$  (Set of all raw prediction tuples  $(o, l, f, c)$ )
3:    $\delta$  (Maximum allowed inconsistency for  $S_{final}$ )
4:    $E_{set}$  (Set of EDR  $\epsilon$  thresholds to evaluate)
5:   {Implicit: Sets  $\mathcal{F}$  (models),  $\mathcal{C}$  (classes); Functions
    $GetFilteredPreds(f, c, \epsilon, P_{raw})$  and  $CalcIncon(S)$ .}
6: Output:  $S_{final}$  (Optimized set of prediction tuples  $(o, l)$ )
7:  $S_{final} \leftarrow \emptyset$ 
8: for each model  $f \in \mathcal{F}$  and class  $c \in \mathcal{C}$  do
9:    $P_{best\_add} \leftarrow \emptyset$  {Best predictions from current  $(f, c)$  to add}
10:   $n_{current\_max} \leftarrow |S_{final}|$  {Max size of  $S_{final} \cup P_{new}$ }
11:  for each  $\epsilon \in E_{set}$  do
12:     $P_{new} \leftarrow GetFilteredPreds(f, c, \epsilon, P_{raw})$ 
13:     $S_{cand} \leftarrow S_{final} \cup P_{new}$ 
14:    if  $CalcIncon(S_{cand}) \leq \delta$  and  $|S_{cand}| > n_{current\_max}$  then
15:       $P_{best\_add} \leftarrow P_{new}$ 
16:       $n_{current\_max} \leftarrow |S_{cand}|$ 
17:    end if
18:  end for
19:  if  $P_{best\_add} \neq \emptyset$  then
20:     $S_{final} \leftarrow S_{final} \cup P_{best\_add}$ 
21:  end if
22: end for
23: return  $S_{final}$ 

```

4.2 Heuristic Search (HS)

Our Heuristic Search (HS) approach is detailed in Algorithm 1. Given the set of all raw model predictions P_{raw} , an inconsistency threshold δ , and a set of EDR ϵ values to evaluate, the algorithm greedily builds a solution S_{final} by iterating through model-class pairs (f, c) . For each pair, it evaluates all ϵ , generating a filtered prediction set P_{new} (via an implicit $GetFilteredPreds(f, c, \epsilon, P_{raw})$ function). It selects the P_{new} that, when added to the current solution S_{final} , maximizes the size of the resulting candidate set $S_{candidate} = S_{final} \cup P_{new}$, while ensuring that $ComputeInconsistency(S_{candidate}) \leq \delta$. This chosen P_{new} for the current (f, c) pair is then added to S_{final} . The HS algorithm has a computational complexity of $O(|\mathcal{F}||\mathcal{C}||E_{set}|)$, where $|\mathcal{F}|$ and $|\mathcal{C}|$ are the numbers of models and classes, and $|E_{set}|$ is the number of evaluated ϵ values—that is, the cost is polynomial with respect to these key parameters of the input. This structured, greedy method efficiently selects predictions while managing inconsistencies, rendering it suitable for large-scale problem instances.

4.3 Tie-Breaker (TB) Mechanism

To ensure a single, deterministic class assignment per object from the solutions generated by our IP and HS approaches, and to resolve ambiguities where multiple class labels might be deemed equally valid post-abduction, we employ a Tie-Breaker (TB) heuristic. This TB mechanism is applied as a refinement step: if an object ω has multiple permissible class labels remaining, the TB heuristic selects the single assignments (ω, c) for which the original perception model that proposed this label reported the highest confidence score. Applying this refinement to the outputs of our core algorithms results in the IP+TB and HS+TB variants evaluated

Table 1: Weather condition intensity distributions for test datasets. Levels: low ([0.0, 0.4]), high ([0.4, 0.6]), uhigh ([0.6, 1]).

id	rain	snow	maple	dust	fog
MDS-A_1	low	low	low	low	low
MDS-A_2	low	low	low	low	low
MDS-A_3	low	low	low	low	low
UM_1	high	low	low	low	low
UM_2	low	low	high	low	low
UM_3	low	low	low	high	low
BM_1	high	low	low	low	high
BM_2	low	high	low	high	low
BM_3	low	low	high	low	high
MM_1	high	high	high	low	low
MM_2	low	high	high	high	low
MM_3	low	high	high	high	low
AM_1	uhigh	uhigh	uhigh	uhigh	uhigh
AM_2	uhigh	uhigh	uhigh	uhigh	uhigh
HUM_1	uhigh	low	low	low	low

in our experiments.

5 Experimental Setup

For evaluating the proposed approaches, we use an extended version of the Multiple Distribution Shift – Aerial (MDS-A) dataset (Ngu et al. 2025). The MDS-A dataset was generated using the AirSim (Shah et al. 2017) simulator and designed to analyze the impact of distributional shifts (caused by varying weather conditions) on object-detection models in aerial imagery. The dataset consists of images (captured in random positions under various weather conditions within a city environment) alongside bounding boxes with one of four categories (pedestrians, vehicles, nature, and construction) assigned to each bounding box. The MDS-A dataset contains six training sets (each simulating a specific weather condition: rain, snow, fog, maple leaves, dust, and a baseline with no weather effects) and three test sets containing a complex mix of weather conditions (Figure 2 illustrates an example of how the intensity distributions of weather effects vary). In addition to the existing test sets, we add an augmented test suite comprising 12 new test sets. These additions introduce a broader range of complex, mixed-weather conditions, further increasing the severity and diversity of distributional shifts. Table 1 presents the configuration of all test datasets. Each entry specifies the intensity level assigned to five different weather conditions, allowing for a systematic exploration of various distributional settings. The suite includes both homogeneous cases—where a single condition dominates—and heterogeneous scenarios involving multiple concurrent weather effects with varying intensities. The id of each dataset refers to the number of weather conditions fitted with the same intensity level: UM (unimodal), BM (bimodal), MM (most models), AM (all models) and HUM (uhigh unimodal). This design aims to evaluate the robustness of the proposed approaches under diverse and increasingly complex distribution shifts.

Six baseline object detection models were trained using the DeTR architecture (Carion et al. 2020) with a ResNet-50 backbone (He et al. 2015), each specialized in

one of the weather-specific training datasets. The models were intentionally trained independently on their corresponding datasets to emphasize the effects of distributional shifts under specific weather conditions. This experimental setup provides a rigorous framework to assess the performance of both the integer programming and heuristic approaches under varying inconsistency thresholds and challenging weather-induced shifts.

Both the integer programming and heuristic approaches were evaluated using a range of inconsistency thresholds, $\delta \in [0.01, 0.1, 0.2, 0.3, 0.4, 0.5, 0.6, 0.7, 0.8, 0.9, 1.0]$. In the case of the heuristic method, the trade-off parameter ϵ was also varied over the same range. Initially, all model-class pairs were included in the optimization process, allowing the heuristic approach to adaptively determine which combinations most effectively improve prediction performance while satisfying the inconsistency constraint. The integer programming formulation followed a similar configuration, incorporating δ as a hard constraint to limit the allowable inconsistencies.

To assess performance, we report the following metrics: *precision*, *recall*, *F1-score*, *accuracy*, and *execution time*—the latter measured as a function of the number of objects present in each analyzed image. The results are compared against three baselines: the majority vote (MV) ensemble method, which selects the most common class prediction across models; the best-performing individual model; and the average performance of all models.

All experiments were conducted on a high-performance computing system, leveraging its advanced computational capabilities. Specifically, we used two configurations: (1) a high-memory node, a Dell PowerEdge R6525 equipped with AMD EPYC 7713 64-Core Processors and 2TB of RAM, and (2) a GPU node, a Dell PowerEdge R7525 with AMD EPYC 7413 24-Core Processors, 512GB of RAM, and three NVIDIA A30 GPUs. The logical deduction process, which applies the learned EDR to raw model outputs to identify *prima facie* predictions and errors, was implemented using PyReason. Subsequently, the IP solutions were implemented using the PuLP library for optimization. The HS approach was implemented in Python, using libraries such as NumPy for efficient computation.

6 Results and Discussion

This section presents the empirical evaluation of our proposed consistency-based abductive reasoning approaches for integrating predictions from multiple models in novel environments. We evaluate their effectiveness and ensure final consistency, including variants that incorporate a tie-break (TB) refinement (IP + TB and HS + TB). The key performance metrics, namely *F1-score* and *Accuracy*, are calculated across the suite of 15 test datasets, encompassing diverse distributional shifts as described in Section 5. Figure 3 (left) summarizes these primary results, providing a comprehensive overview of how each method performs under various challenging conditions.

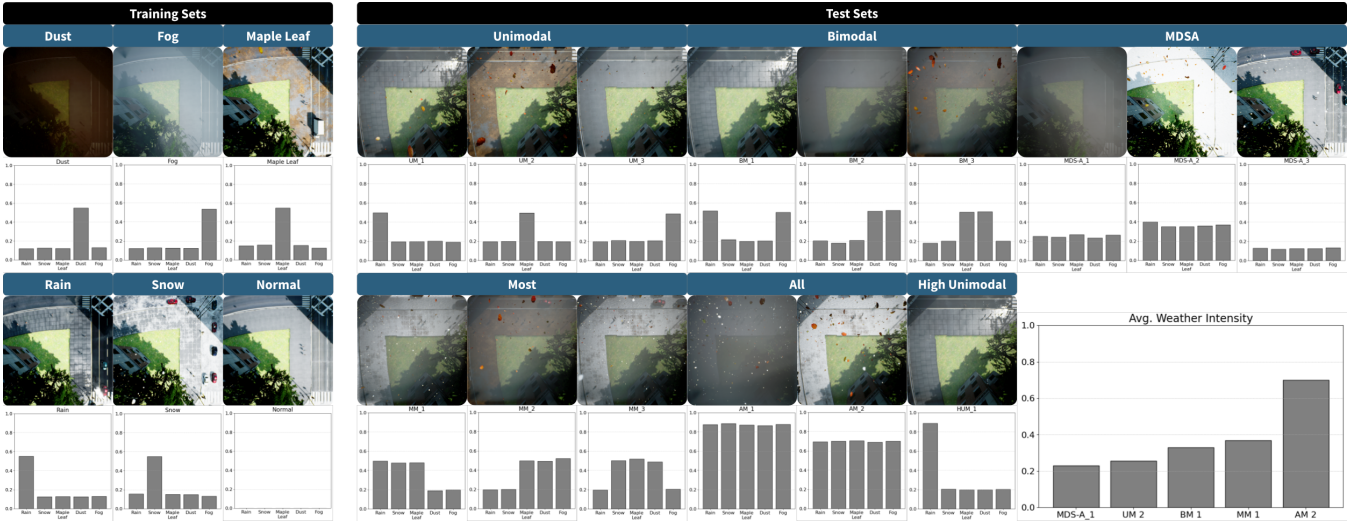


Figure 2: Images captured in the same position in AirSim under various weather conditions along with histograms showing the distribution of weather conditions of the dataset that it represents. Bottom right is a histogram showing the average of intensity of some datasets.

6.1 Overall Performance Analysis

Examining the F1-score and Accuracy metrics, the IP + TB method consistently demonstrates superior performance, achieving the highest scores in all cases. For instance, on the challenging AM_1, AM_2, and HUM_1 test sets, characterized by significant distributional shifts, IP + TB yields notable improvements over the best-performing individual model and significantly surpasses the standard Majority Vote (MV) ensemble, which often struggles in these complex scenarios (e.g., F1 scores of 0.21 vs. 0.18 vs. 0.05 on AM_1). The heuristic approach, HS + TB, also frequently outperforms the baselines, achieving for example the second-best F1 and Accuracy on the UM_1 test set (F1 0.61, Acc 0.44) and demonstrating strong performance on others like MDS-A_1. These results highlight the effectiveness of combining consistency-based abduction with a tie-breaking mechanism that selects the highest confidence prediction among inconsistent options. The contribution of this tie-breaker component is further analyzed in the ablation study presented in Subsection 6.3.

6.2 Performance Across Varying Environmental Intensity

To assess the robustness of our proposed methods against increasing environmental challenge, Figure 4 displays the F1-score for all 15 test datasets plotted against their average environmental intensity. Each point represents a unique test set, with different markers indicating the performance of IP+TB, HS+TB, and the baseline methods (Best Individual Model, Average Models, and Majority Vote). The average environmental intensity for each dataset (x-axis) is a normalized measure reflecting the severity of simulated conditions.

As observable in Figure 4, while there is a general trend of decreasing F1-scores for all methods as the average environmental intensity increases—indicating the inherent difficulty of operating in more severe novel environments—our

IP+TB approach (represented by red diamonds) consistently achieves the highest F1-scores across the entire spectrum of intensities. In nearly all instances, IP+TB surpasses the Best Individual Model, and significantly outperforms the Average Models, Majority Vote, and our Heuristic Search (HS+TB) approach in terms of F1-score. This consistent superiority, irrespective of the environmental intensity level, underscores the effectiveness of IP+TB in robustly integrating model predictions and managing inconsistencies. For instance, even at higher intensity levels where all methods experience performance degradation, IP+TB maintains a clear advantage. The same analysis for Accuracy shows comparable trends, and is provided in the supplementary material.

These findings demonstrate that while environmental novelty impacts all approaches, our consistency-based abductive reasoning, particularly when implemented via Integer Programming (IP+TB), provides a robust performance advantage in F1-score over baseline methods and our heuristic alternative across a wide range of challenging conditions.

6.3 Ablation Study: Impact of Tie-Breaker

To evaluate the Tie-Breaker (TB) mechanism’s role in ensuring consistent final predictions and its effect on performance, we carried out an ablation study comparing results with TB (Figure 3-left) and without TB (summarized in Figure 3-right, showing percentage differences). For the Integer Programming (IP) approach, removing the TB resulted in a 0.0% difference in performance across all metrics and datasets. This is a notable outcome. It suggests that for the chosen optimal δ values (typically in the range of 0.1 to 0.3, as per our sensitivity analysis in Subsection 6.5), the IP optimization, in its pursuit of maximizing valid assignments inherently converged to solutions that were already fully consistent in term of providing a single, unambiguous label per object, or where any minor ambiguities were resolvable by the TB without affecting the F1-score or Acc-

Test Set	Best		Avg.		MV		IP+TB		HS+TB	
	F1	Acc	F1	Acc	F1	Acc	F1	Acc	F1	Acc
MDS-A_1	<u>0.57</u>	0.40	0.52	0.36	0.28	0.34	0.58	0.41	0.58	0.41
MDS-A_2	<u>0.33</u>	0.20	0.29	0.17	0.26	0.22	0.37	0.22	0.32	0.19
MDS-A_3	0.54	0.37	0.49	0.33	0.39	0.29	0.56	0.39	<u>0.55</u>	0.38
UM_1	0.54	0.37	0.47	0.31	0.26	0.23	0.64	0.47	<u>0.61</u>	0.44
UM_2	0.56	0.38	0.46	0.31	0.25	0.22	0.64	0.47	<u>0.61</u>	0.44
UM_3	0.54	0.37	0.43	0.28	0.22	0.19	0.63	0.46	<u>0.59</u>	0.42
BM_1	<u>0.42</u>	0.27	0.33	0.20	0.19	0.16	0.45	0.29	0.39	0.24
BM_2	0.33	0.20	0.25	0.15	0.14	0.12	0.37	0.23	<u>0.36</u>	0.22
BM_3	0.37	0.23	0.31	0.19	0.18	0.16	0.43	0.27	<u>0.40</u>	0.25
MM_1	<u>0.46</u>	0.30	0.40	0.25	0.22	0.21	0.51	0.34	<u>0.46</u>	0.30
MM_2	<u>0.32</u>	0.19	0.24	0.14	0.13	0.10	0.36	0.22	0.29	0.17
MM_3	<u>0.41</u>	0.26	0.35	0.22	0.18	0.16	0.46	0.30	0.39	0.24
AM_1	<u>0.18</u>	0.10	0.12	0.07	0.05	0.04	0.21	0.11	<u>0.18</u>	0.10
AM_2	<u>0.23</u>	0.13	0.18	0.10	0.07	0.06	0.28	0.16	<u>0.23</u>	0.13
HUM_1	0.45	0.29	0.40	0.25	0.18	0.17	0.57	0.40	<u>0.55</u>	0.38

Test Set	IP (No TB)		HS (No TB)	
	F1 (% Diff)	Acc (% Diff)	F1 (% Diff)	Acc (% Diff)
MDS-A_1	0.58 (0.0)	0.41 (0.0)	0.52 (-10.3%)	0.35 (-14.6%)
MDS-A_2	0.37 (0.0)	0.22 (0.0)	0.27 (-15.6%)	0.16 (-16.7%)
MDS-A_3	0.56 (0.0)	0.39 (0.0)	0.49 (-10.9%)	0.32 (-15.8%)
UM_1	0.64 (0.0)	0.47 (0.0)	0.53 (-13.1%)	0.36 (-18.2%)
UM_2	0.64 (0.0)	0.47 (0.0)	0.52 (-14.1%)	0.35 (-18.8%)
UM_3	0.63 (0.0)	0.46 (0.0)	0.52 (-11.9%)	0.35 (-16.7%)
BM_1	0.45 (0.0)	0.29 (0.0)	0.34 (-11.1%)	0.20 (-16.7%)
BM_2	0.37 (0.0)	0.23 (0.0)	0.31 (-13.5%)	0.19 (-13.6%)
BM_3	0.43 (0.0)	0.27 (0.0)	0.34 (-15.0%)	0.20 (-20.0%)
MM_1	0.51 (0.0)	0.34 (0.0)	0.38 (-15.7%)	0.24 (-20.0%)
MM_2	0.36 (0.0)	0.22 (0.0)	0.25 (-13.8%)	0.14 (-17.6%)
MM_3	0.46 (0.0)	0.30 (0.0)	0.33 (-15.4%)	0.20 (-16.7%)
AM_1	0.21 (0.0)	0.11 (0.0)	0.15 (-16.7%)	0.08 (-20.0%)
AM_2	0.28 (0.0)	0.16 (0.0)	0.19 (-17.4%)	0.11 (-15.4%)
HUM_1	0.57 (0.0)	0.40 (0.0)	0.48 (-12.7%)	0.32 (-15.8%)

Figure 3: *Left:* Performance (F1 and Accuracy) across all test sets. *Right:* Ablation Study – Performance without Tie-Breaker (TB). Values show F1-score or Accuracy for the method without TB, with the percentage difference relative to the corresponding + TB version (from the table on the left shown in parentheses).

Best values per test set in bold, the second-best are underlined. This parameter controls the aggressiveness of filtering potentially erroneous predictions from individual models before the main abduction process. Figure 5 (top-left) illustrates the typical impact of varying ϵ on precision, recall, F1-score, and the inconsistency rate (i.e., conflicting predictions) for the MDS-A_1 test set.

As expected, increasing ϵ generally leads to higher precision but lower recall, demonstrating the inherent trade-off controlled by this parameter. Notably, this stricter filtering also tends to reduce the baseline level of inconsistency among the remaining predictions. This analysis highlights how tuning ϵ shapes the pool of candidate predictions subsequently processed by our IP+TB and HS+TB abduction methods aiming to maximize valid assignments under the global inconsistency constraint δ . Detailed sensitivity plots for all test sets are provided in the supplementary material.

6.5 Hyperparameter Sensitivity (ϵ, δ)

We analyzed the sensitivity of our approaches to the maximum inconsistency threshold hyperparameter δ , which applies to IP+TB and HS+TB, and the internal recall parameter ϵ used within the IP+TB optimization. Figure 5 (bottom) illustrates this sensitivity analysis for the MDS-A_1 test set. The 3D plots of IP+TB show that the F1 score and accuracy reach their maximum value in the ranges of δ between 0.1, and 0.3 and for ϵ in 0.1 and 0.5. Similarly, the performance of HS+TB (top-right) stabilizes quickly as δ increases above a small initial value (e.g., 0.2), which is associated with the maximum level of inconsistency present in the initial test set (Figure 5, top-left). Detailed sensitivity plots for all test sets are provided in the supplementary material.

6.6 Running Time Analysis and Complexity

A key practical difference lies in the computational cost. Figure 6 illustrates the average running times for IP+TB, HS+TB and MV, as a function of the number of objects. This empirical observation of running time performance

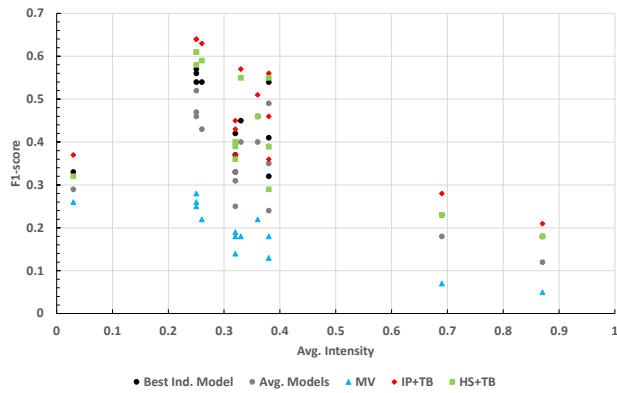


Figure 4: Scatter plot of F1-scores for the proposed methods (IP+TB, HS+TB) against baselines (Best Ind. Model, Avg. Models, and Majority Vote) across all 15 test datasets under increasing average weather intensity.

accuracy. Thus, the IP approach effectively achieved a high degree of output consistency by primarily leveraging other aspects of the formulation, such as the elimination of less reliable model-class pairs, potentially rendering the solution more consistent than strictly required by the explicit δ budget for conflicting assignments. In contrast, the Heuristic Search (HS) performance degraded consistently without the TB. As shown by the negative percentage differences in Figure 3 (right), the F1-score for HS dropped by 10% to over 17% across various datasets when the TB was removed, with similar reductions in Accuracy. Recall that the tie-breaker heuristic selects the highest confidence prediction when an inconsistency is present.

6.4 Impact of Error Detection Rule Strictness

We also analyze the sensitivity of the initial Error Detection Rule (EDR) learning stage to its recall reduction threshold ϵ .

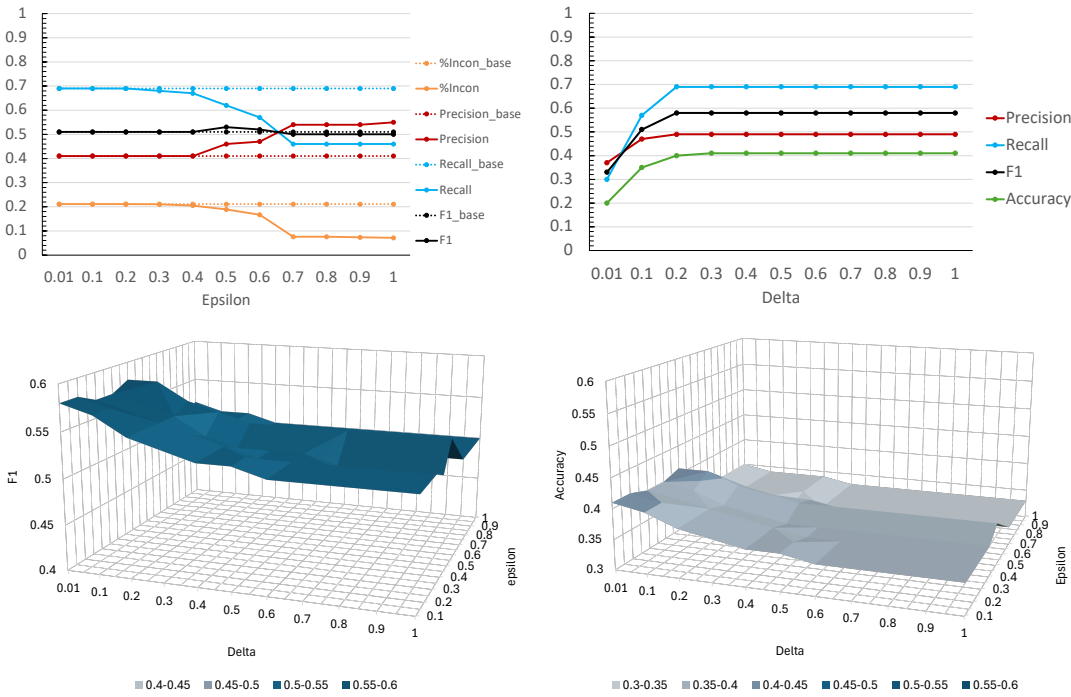


Figure 5: Hyperparameter sensitivity analysis for the MDS-A.1 test set. (Top-left): Performance metrics and inconsistency rates of the Error Detection Rule (EDR) stage across varying Epsilon (ϵ) values. (Top-right): Heuristic Search (HS+TB) performance, as a function of the inconsistency threshold Delta (δ). (Bottom-left): IP+TB F1-score shown as a surface plot dependent on threshold δ and its internal optimization ϵ . (Bottom-right): IP+TB Accuracy depicted as a surface plot, varying with δ and internal ϵ

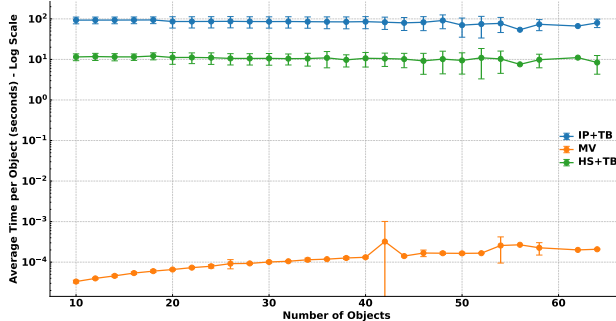


Figure 6: Average running time by number of objects (all test sets)

is well-aligned with the theoretical complexity of the two approaches. The runtime for the IP+TB approach, while higher due to its exact optimization nature, was found to be tractable for the problem instances explored in our experiments. Nevertheless, the inherent computational demands to guarantee optimality with IP are typically higher than those of polynomial-time heuristics like our HS approach.

The running time plot for IP+TB (Figure 6) shows that the average processing time per object does not exhibit a steep increase and, in some ranges, may appear to plateau or even slightly decrease as the total number of objects grows. Regarding this trend, we hypothesize that it may stem from a combination of factors. Firstly, the amortization of fixed

computational overheads associated with solver initialization and the presolve phase becomes more pronounced over a larger number of objects. Secondly, as the plotted values represent averages across all diverse test sets, specific dataset characteristics can significantly influence this aggregated trend. Indeed, as detailed in our supplementary material where running times are disaggregated by individual test sets, datasets such as MDS-A.2, UM_1, and BM_3 particularly contribute to this observation by exhibiting comparatively lower average processing times per object for IP+TB. This suggests that these specific datasets might have structural characteristics (e.g., lower initial conflict density among base model predictions or a simpler path to an optimal consistent solution) that make them intrinsically faster for the IP solver on a per-object basis, thereby influencing the overall average. A more detailed investigation into these nuanced runtime dynamics, disentangling the effects of object quantity from specific dataset complexities, constitutes an important avenue for future work. The aforementioned per-dataset running time breakdowns in the supplementary material provide further evidence for these observations.

7 Conclusions and Future Work

In this work, we presented a comprehensive approach to address inconsistencies in model predictions through heuristic and logic programming solutions. In future work, we plan to focus on the logic program for the deduction process to

incorporate more sophisticated rules to infer alternative sets of assignments that address diverse inconsistency scenarios among model predictions. These enhancements will be applied to new domains and datasets characterized by complex distributions. Furthermore, we plan to refine our analysis by carrying out a more granular exploration of values of both the ϵ and δ parameters in order to evaluate the impact on solution robustness. Finally, optimizing runtime efficiency remains a priority to enable scalability and practical application of our approach in real-world scenarios.

Acknowledgments

This research was supported by the Defense Advanced Research Projects Agency (DARPA) under Cooperative Agreement No. HR00112420370 (MCAI). The views expressed in this paper are those of the authors and do not necessarily reflect the official policy or position of the U.S. Military Academy, the U.S. Army, the U.S. Department of Defense, or the U.S. Government.

References

Aditya, D.; Mukherji, K.; Balasubramanian, S.; Chaudhary, A.; and Shakarian, P. 2023. Pyreason: Software for open world temporal logic.

Akyürek, E.; Damani, M.; Qiu, L.; Guo, H.; Kim, Y.; and Andreas, J. 2024. The surprising effectiveness of test-time training for abstract reasoning.

Carion, N.; Massa, F.; Synnaeve, G.; Usunier, N.; Kirillov, A.; and Zagoruyko, S. 2020. End-to-end object detection with transformers.

Cheng, G., and Han, J. 2016. A survey on object detection in optical remote sensing images. *ISPRS journal of photogrammetry and remote sensing* 117:11–28.

Dai, W.-Z.; Xu, Q.; Yu, Y.; and Zhou, Z.-H. 2019. Bridging machine learning and logical reasoning by abductive learning. *Advances in Neural Information Processing Systems* 32.

Gabbay, D. M., and Smets, P. 2013. *Abductive reasoning and learning*, volume 4. Springer Science & Business Media.

Han, X.; Zhang, Z.; Ding, N.; Gu, Y.; Liu, X.; Huo, Y.; Qiu, J.; Yao, Y.; Zhang, A.; Zhang, L.; et al. 2021. Pre-trained models: Past, present and future. *AI Open* 2:225–250.

He, K.; Zhang, X.; Ren, S.; and Sun, J. 2015. Deep residual learning for image recognition.

Huang, Y.-X.; Dai, W.-Z.; Jiang, Y.; and Zhou, Z.-H. 2023. Enabling knowledge refinement upon new concepts in abductive learning. *Proceedings of the AAAI Conference on Artificial Intelligence* 37(7):7928–7935.

Johnson, S. G. B.; Karimi, A.-H.; Bengio, Y.; Chater, N.; Gerstenberg, T.; Larson, K.; Levine, S.; Mitchell, M.; Rahwan, I.; Schölkopf, B.; and Grossmann, I. 2024. Imagining and building wise machines: The centrality of AI Metacognition.

Kifer, M., and Subrahmanian, V. 1992. Theory of generalized annotated logic programming and its applications. *The Journal of Logic Programming* 12(4):335–367.

Kricheli, J. S.; Vo, K.; Datta, A.; Ozgur, S.; and Shakarian, P. 2024. Error detection and constraint recovery in hierarchical multi-label classification without prior knowledge. In *Proceedings of the 33rd ACM International Conference on Information and Knowledge Management*, 3842–3846.

Lee, N.; Ngu, N.; Sahdev, H. S.; Motaganahall, P.; Chowdhury, A. M. S.; Xi, B.; and Shakarian, P. 2024. Metal price spike prediction via a neurosymbolic ensemble approach. In *2024 IEEE International Conference on Data Mining Workshops (ICDMW)*.

Ngu, N.; Taparia, A.; Simari, G. I.; Leiva, M.; Corcoran, J.; Senanayake, R.; Shakarian, P.; and Bastian, N. D. 2025. Multiple distribution shift – aerial (mds-a): A dataset for test-time error detection and model adaptation. In *AAAI Spring Symposium*.

Parisi, S.; Rajeswaran, A.; Purushwalkam, S.; and Gupta, A. 2022. The unsurprising effectiveness of pre-trained vision models for control. In *international conference on machine learning*, 17359–17371. PMLR.

Poole, D. 1989. Normality and faults in logic-based diagnosis. In *Proceedings of the 11th International Joint Conference on Artificial Intelligence - Volume 2*, IJCAI'89, 1304–1310. San Francisco, CA, USA: Morgan Kaufmann Publishers Inc.

Shah, S.; Dey, D.; Lovett, C.; and Kapoor, A. 2017. Airsim: High-fidelity visual and physical simulation for autonomous vehicles. In *Field and Service Robotics*.

Shakarian, P.; Simari, G. I.; and Bastian, N. D. 2025. Probabilistic foundations for metacognition via hybrid-ai.

Sun, Y.; Wang, X.; Zhuang, L.; Miller, J.; Hardt, M.; and Efros, A. A. 2020. Test-time training with self-supervision for generalization under distribution shifts. In *ICML*.

Sutor, P.; Yuan, D.; Summers-Stay, D.; Fermuller, C.; and Aloimonos, Y. 2022. Gluing neural networks symbolically through hyperdimensional computing. In *2022 International Joint Conference on Neural Networks (IJCNN)*, 1–10. IEEE.

Wei, H.; Shakarian, P.; Lebriere, C.; Draper, B. A.; Krishnaswamy, N.; and Nirenburg, S. 2024. Metacognitive AI: framework and the case for a neurosymbolic approach. In Besold, T. R.; d'Avila Garcez, A.; Jiménez-Ruiz, E.; Confalonieri, R.; Madhyastha, P.; and Wagner, B., eds., *Neural-Symbolic Learning and Reasoning - 18th International Conference, NeSy 2024, Barcelona, Spain, September 9-12, 2024, Proceedings, Part II*, volume 14980 of *Lecture Notes in Computer Science*, 60–67. Springer.

Xi, B.; Scaria, K.; Bavikadi, D.; and Shakarian, P. 2024. Rule-based error detection and correction to operationalize movement trajectory classification.